RESEARCH ARTICLE | JULY 03 2025

Microstructure and super-high coercivity of Tb-containing NdFeB magnets by diffusion with Tb metal and Pr-Al-Cu-Ga

Jianlong Fu ; Dongbo Wang ; Yan Gao; Haiyang Yu; Deying Zhu; Yanwei Song; Kai Qu; Wenliang Xie; Yu Wang; Guozheng Liu

AIP Advances 15, 075206 (2025)
https://doi.org/10.1063/5.0273816

Microstructure and super-high coercivity of Tb-containing NdFeB magnets by diffusion with Tb metal and Pr-Al-Cu-Ga

Cite as: AIP Advances 15, 075206 (2025); doi: 10.1063/5.0273816
Submitted: 2 April 2025 • Accepted: 12 June 2025 •
Published Online: 3 July 2025

Jianlong Fu,[a] Dongbo Wang,[a] Yan Gao, Haiyang Yu, Deying Zhu, Yanwei Song, Kai Qu, Wenliang Xie, Yu Wang, and Guozheng Liu

AFFILIATIONS

State Key Laboratory of Baiyunobo Rare Earth Resource Researches and Comprehensive Utilization, Baotou Research Institute of Rare Earths, Baotou 014030, People's Republic of China and Baotou Research Institute of Rare Earths, Baotou 014030, People's Republic of China

[a]**Authors to whom correspondence should be addressed:** fujianlong@brire.com and wangdongbo@brire.com

ABSTRACT

A sintered NdFeB magnet with super-high coercivity of 46.21 kOe was successfully obtained by two-step diffusion with Tb metal and Pr-Al-Cu-Ga alloys. Tb-containing magnets with super-high coercivity were used as base magnets; coercivity increased from 35.86 to 44.51 kOe for the Tb-diffused magnet and 46.21 kOe for the magnet with Tb and Pr-Al-Cu-Ga diffusion. Microstructure analysis indicated that two-step diffusion resulted in Tb/Pr-rich double-shell structures, optimized grain boundary structure, and the enhancement of RE-rich grain boundary phases, which is the main reason for the enhancement of coercivity. The diffusion-induced variation of remanence was also discussed. This work provides insights into further breaking the coercivity limit of sintered NdFeB magnets.

INTRODUCTION

Sintered NdFeB magnets with super-high coercivity have been widely used in various permanent magnet traction motors.[1,2] For example, the coercivity of Nd-Fe-B magnets in the traction motors of electric vehicles exceeds 3 T[3]. In view of the working temperature of the magnet in the traction motor reaching 200 °C or above,[3] it is very important to ensure the high temperature stability of the magnet. The key to resisting thermal demagnetization at high temperature is to improve the initial coercivity of the magnet at room temperature. At present, the modification of magnets by the grain boundary diffusion process of heavy rare earth elements (HRE, Tb/Dy) has become the key technology path to significantly improve the coercivity. Grain boundary diffusion technology enhances the demagnetization coupling between neighboring matrix-phase grains by increasing the proportion of grain boundary phases, optimizing the distribution of grain boundary phase, and improving the continuity of grain boundary phases.[4] HRE atoms replacing Pr/Nd atoms can form HRE-rich shell structures on the surface of the matrix-phase grains, and the nucleation and expansion of the magnetized domains are inhibited by the stronger magnetocrystalline anisotropy of the shell.[5] This method can improve the coercivity of sintered NdFeB magnets without significant loss of remanence and has high utilization rate of heavy rare earth metals.

With the development of high-speed permanent magnet traction motors in the field of new energy vehicles and rail transit, the coercivity of sintered NdFeB magnets must be further improved. Recently, groundbreaking research has been conducted in the field of super-high coercivity magnets. Hu *et al.* reported that the coercivity of the magnet was increased from 31.6 to 35.2 kOe by coating Dy alloy powder on the surface of the magnet for grain boundary diffusion treatment, improving the distribution and continuity of grain boundary phases and increasing the magnetocrystalline anisotropy field on the surface of the grain.[6] Zhang *et al.* studied that TbH_x powders were coated on the surface of the magnet for grain boundary diffusion treatment.[7] The morphology of the

surface grain near the magnet was consistent with that of the central grain, and the surface of the grain was flat. When the weight gain of Tb reached 1.66%, the coercivity of the magnet increased from 31.70 to 43.34 kOe. Zhou *et al.* prepared base magnets with initial Tb-poor shells from low Dy/Tb matrix-phase alloys and Tb-rich matrix-phase alloys by double alloy methods, and then, Tb-Cu-Ga alloys were diffused to form RE-(Fe, CuGaO) grain boundary layers and Tb-poor and Tb-rich double-shell structures.[8] The Tb-rich shell can prevent the expansion of the reverse magnetization domain in the Tb-poor shell region and finally the coercivity of the magnet increased to 35.46 kOe. Wu *et al.* reported that TbH_3 nanoparticles were coated on the surface of the magnet for grain boundary diffusion treatment, and the core/shell type rare-earth element distribution appeared on the surface of the matrix-phase grains, leading to an increase in the coercivity of the magnet from 34.8 to 47.1 kOe.[9] Jia *et al.* prepared high-performance base magnets, utilizing B-rich phase and Pr-Tb-Fe auxiliary alloy to form high concentration Tb segregation zone and Pr-rich shells through the micrometallurgical reaction at the grain boundary.[10] Then, TbH_x powders and Pr-Fe-Al-Ga alloys were step-by-step diffused to form Tb-rich shells and Pr-rich shells, achieving matrix-phase grains with double shells, and finally, the coercivity of the magnet reached 44.21 kOe.

The recent results show that the conventional HRE grain boundary diffusion has some limitations. The diffusion depth of HRE in the magnet is limited, which cannot be effectively solved even by prolonging the time or increasing the temperature.[11,12] In addition, the simulation results show that coercivity of the magnet tends to be saturated when the shell thickness exceeds 15 nm.[13,14] Therefore, the two-step diffusion process has become one of the most potential technical paths to break through the limit of super-high coercivity. In this paper, we first prepared Tb-containing sintered NdFeB base magnets with super-high coercivity, and then, the coercivity of the magnet was incrementally raised by two-step diffusion of Tb metal and Pr-Al-Cu-Ga alloys. In addition, the effects of microstructures and grain boundary phase changes on the magnetic properties of the magnet were systematically studied.

EXPERIMENTAL

The strip cast Tb-containing alloy with the nominal composition of $(PrNd)_{25.5}Tb_{4.5}FebalB_{1.0}M_{1.5}$ (M = Cu, Al, Co, Ga, wt. %) was subjected to hydrogen decrepitation and N_2-jet milling process to produce powders of average particle size 3.0 μm. The fine powders were compacted at the DC magnetic field of 2.0 T and cold isostatic-pressed at the pressure of 200 MPa. The obtained greens were sintered at 1080 °C for 3 h and then subjected to two-step annealing at 900 °C for 1.5 h and 500 °C for 3 h in vacuum and named the original magnet. Pr_{70} $Al_{15}Cu_{10}Ga_5$ (at. %) (defined as PACG) ingots were produced by arc melting and then cut into Ø10 mm circular slices using the wire electrode cutting method. The as-sintered magnet was cut into Ø10 × 3 mm^2 cylinders as the base magnets. Both the magnet and the PACG slices were polished, followed by ultrasonic cleaning with alcohol. The base magnets were placed in a multi-arc ion plating machine with Tb targets (purity: >99.99%); Tb coating thickness on both the top and bottom surfaces was 8 μm. After diffusion at 930 °C for 3 h in vacuum, the magnet was polished and cleaned to remove impurities. This magnet was named T-GBD magnet. The upper and lower surfaces of the T-GBD magnet were covered with PACG slices and then subjected to two-step heating at 930 °C for 3 h and 500 °C for 3 h in vacuum. This magnet was named TP-GBD magnet.

The demagnetization curves at 20 °C were measured using a pulsed field magnetometer (PFM, PFM14.cn), and the microstructure and elemental concentration mapping were performed using an electron probe microanalyzer (EPMA). The phase analysis was conducted by x-ray diffraction (XRD) using a Philips diffractometer with Cu-Kα radiation.

RESULTS AND DISCUSSION

Table I displays the magnetic properties of magnets, and the demagnetization curves of magnets are shown in Fig. 1. The coercivity (H_{cj}) of the original magnet is 35.86 kOe, the remanence (B_r) is 12.88 kGs, and the maximum energy product [$(BH)_{max}$] is 40.11 MGOe. After grain boundary diffusion of Tb metal, the coercivity of the T-GBD magnet is significantly enhanced to 44.51 kOe. Then, after grain boundary diffusion of PACG alloys, the coercivity of the TP-GBD magnet is further enhanced to 46.21 kOe. The remanence of both GDB-treated magnets decreased, and finally, the remanence loss of the TP-GBD magnet is 0.36 kGs. Importantly, after coercivity enhancement via Tb diffusion reaches its limit, the diffusion of PACG can further improve coercivity. It indicates that two-step diffusion facilitates the maximization of coercivity.

Figures 2 and 3 shows BSE-SEM images and the element distribution of Tb, Pr, and Nd at different depths below the surface

TABLE I. Magnetic properties of the original magnet, T-GBD magnet, and TP-GBD magnet.

Samples	B_r (kGs)	H_{cj} (kOe)	$(BH)_{max}$ (MGOe)
Original	12.88	35.86	40.11
T-GBD	12.70	44.51	39.50
TP-GBD	12.52	46.21	38.31

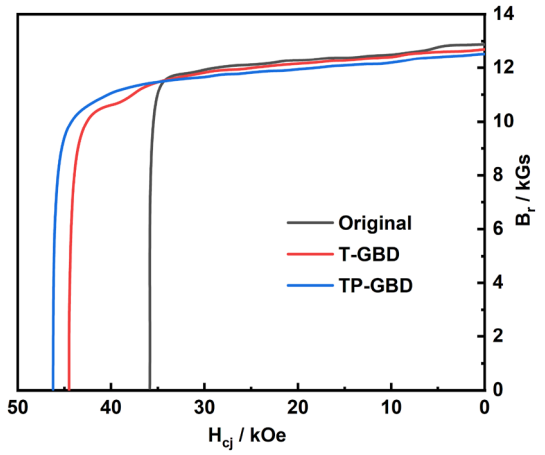

FIG. 1. Demagnetization curves of the original magnet, T-GBD magnet, and TP-GBD magnet.

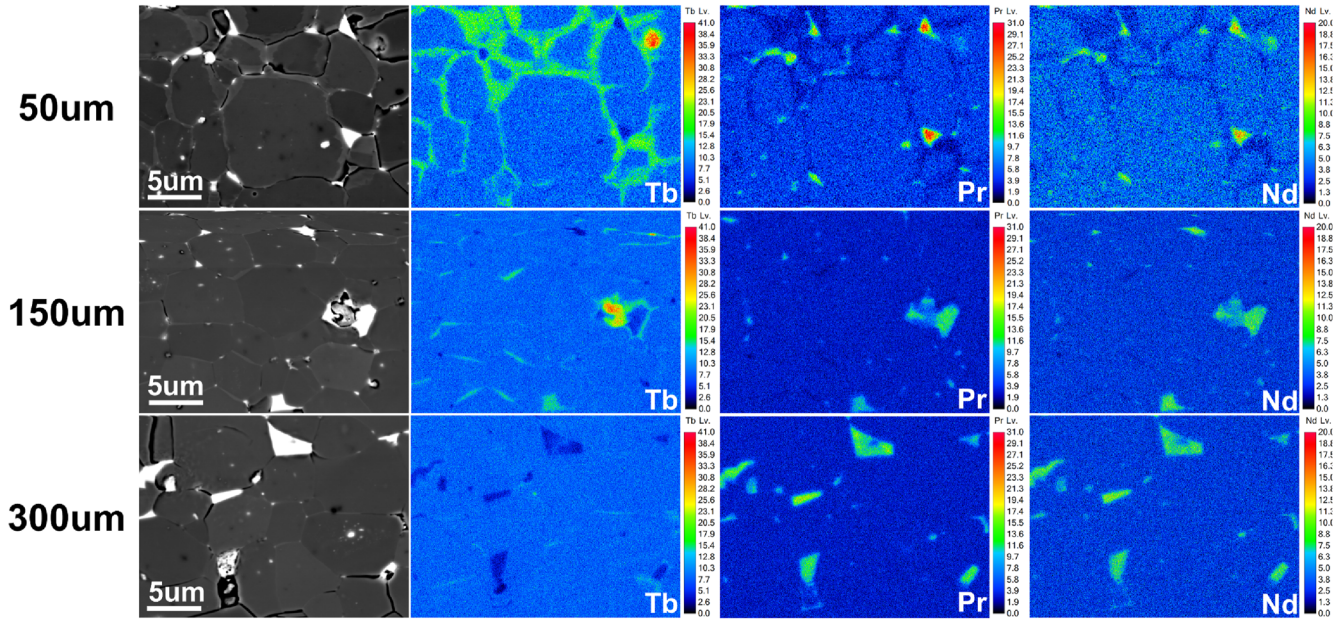

FIG. 2. BSE-SEM images and the element distribution of Tb, Pr, and Nd at 50 μm, 150 μm, and 300 μm below the surface of the T-GBD magnet.

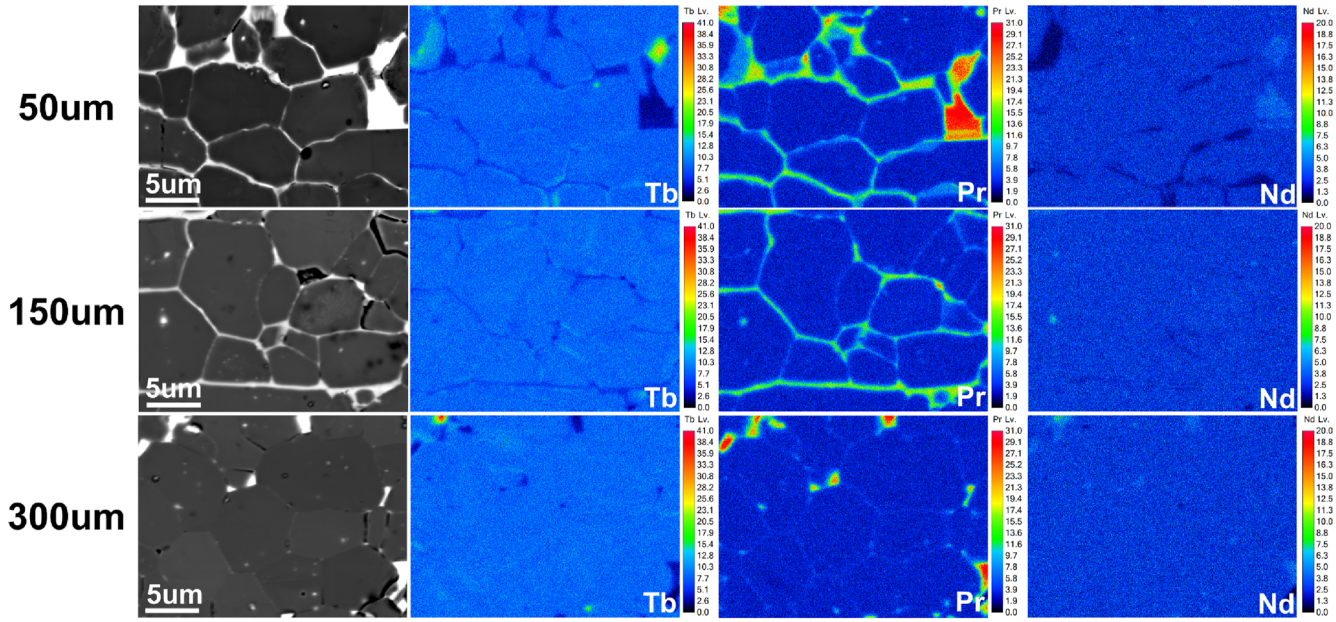

FIG. 3. BSE-SEM images and the element distribution of Tb, Pr, and Nd at 50 μm, 150 μm, and 300 μm below the surface of the TP-GBD magnet.

of the T-GBD magnet and TP-GBD magnet by EPMA. As for the T-GBD magnet (Fig. 2), the typical core–shell structures can be clearly observed in BSE-SEM images and it becomes less distinct at 300 μm. In detail, Tb-rich shells were formed according to the mapping of Tb, and as the depth increases, the Tb-rich shell becomes thinner. After diffusion of Tb metal, Tb atoms partially replace the Pr/Nd atoms, forming Tb-rich shells on the surface layer of the matrix-phase grains. The Tb-rich shell exhibits higher magnetocrystalline anisotropy, which contributes to the enhancement of coercivity.[15] As for the TP-GBD magnet (Fig. 3), the continuous and thin grain boundaries can be clearly observed at 50 and 150 μm, while the grain boundaries at 300 μm becomes very thin.

It can be seen that the thicknesses of the Tb-rich shells of the TP-GBD magnets become drastically thinner at 50 μm compared to the T-GBD magnet. Network-like Pr-rich grain boundaries can be observed at 50 and 150 μm in the TP-GBD magnets. During diffusion of PACG alloys, Tb atoms in Tb-rich shells partially are replaced by the Pr atoms in PACG alloys, leading to decreased thicknesses of the Tb-rich shells and then forming Pr-rich shells on the surface layer of the matrix-phase grains. Thus, there are Tb-rich and Pr-rich double-shell structures in the TP-GBD magnet. The double-shell structures can prevent the expansion of reversed domain, facilitating the enhancement of coercivity.[8,10] In addition, the Pr-rich grain boundaries can enhance the demagnetizing coupling between neighboring matrix-phase grains, which is also beneficial for enhancing coercivity.[16,17]

Figure 4 shows BSE-SEM images and the element distribution of Cu, Al, and Ga at 50 μm below the surface of the T-GBD magnet and TP-GBD magnet by EPMA. Compared to the T-GBD magnet, more elements of Cu, Al, and Ga are enriched at the grain boundaries in the TP-GBD magnet, especially Al elements partly diffused into the matrix-phase grains. Elements of Cu, Al, and Ga at the grain boundaries can improve grain boundary wettability and optimize grain boundary structure, which is beneficial for enhancing coercivity.[18,19] Furthermore, the enhancement of the RE-rich grain boundary phase can also enhance coercivity.[4] However, due to the higher solubility of Al in the matrix-phase grains, Al tends to diffuse into the matrix-phase grains, leading to a reduction in the saturation magnetization and anisotropy field of the matrix-phase grains, thereby deteriorating the magnetic properties.[20,21]

Figure 5 shows XRD patterns of the original magnet, T-GBD magnet, and TP-GBD magnet. All magnets exhibit strong c-axis alignment as a result of dominant reflection peaks of (00L) and (105). The intensity ratios (R) of (006) to (105) peaks are used to quantitatively characterize the orientation degree for NdFeB magnets, that is, $R = I_{(006)}/I_{(105)}$[8]. The R value of the T-GBD magnet is 1.34, which is less than 1.44 of the original magnet. It indicates that the diffusion of Tb metal resulted in a decrease in the degree of orientation. Then, the degree of orientation remained essentially unchanged after diffusion of PACG alloys. As shown in the magnified micrograph of reflection peaks of (006), the reflection peak of (006) is shifted toward higher angle after diffusion of Tb metal, corresponding to the formation of the Tb-rich shell in the EPMA result. The atomic radius of Pr (1.82 Å) is larger than that of Tb (1.77 Å), leading to reduction in the crystal plane spacing.[10,22] In addition, the reflection peak of (006) is shifted toward a lower angle after diffusion of PACG alloys, indicating that Tb atoms in Tb-rich shells are replaced by the Pr atoms, consistent with the EPMA result. Hence, loss of remanence resulting from the diffusion of Tb metal may be attributed to the decreased degree of orientation and the less saturation magnetization of the Tb-rich shell.[23–25] Integrating the EPMA result, loss of remanence resulting from the diffusion of PACG alloys should be attributed to the enhancement of RE-rich grain boundary phases and the diffusion of Al into the matrix-phase grains.[26,27]

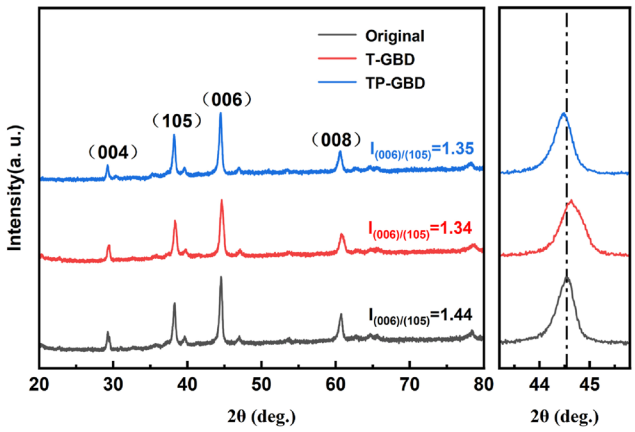

FIG. 5. XRD patterns of the original magnet, T-GBD magnet, and TP-GBD magnet.

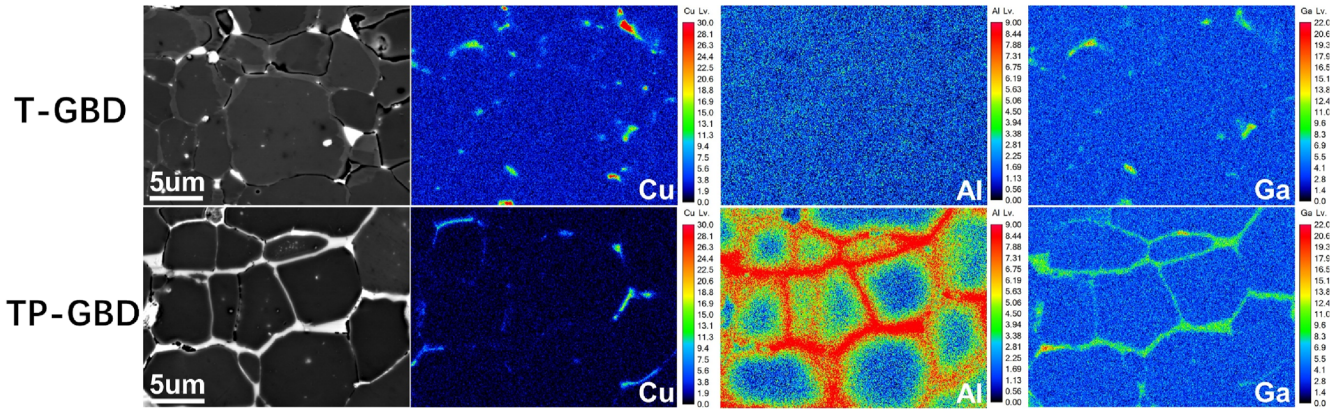

FIG. 4. BSE-SEM images and the element distribution of Cu, Al, and Ga at 50 μm below the surface of the T-GBD magnet and TP-GBD magnet.

CONCLUSION

In summary, a sintered NdFeB magnet with super-high coercivity of 46.21 kOe was successfully obtained. Tb-containing base magnets with super-high coercivity were incrementally raised by two-step diffusion with Tb metal and PACG alloys. Microstructure analysis indicated that the super-high coercivity of the final magnet should be attributed to Tb/Pr-rich double-shell structures, optimized grain boundary structure, and the enhancement of RE-rich grain boundary phases. This work provides insights into further breaking the coercivity limit of sintered NdFeB magnets.

ACKNOWLEDGMENTS

This work was supported by the Key Science and Technology Special Project of Inner Mongolia Autonomous Region (Grant Nos. 2021ZD0035 and 2019ZD020), the Foundation of State Key Laboratory of Baiyunobo Rare Earth Resource Researches and Comprehensive Utilization (Grant No. 2022H2385-1), the National Key Research and Development Program of China (Grant No. 2022YFB3503401), and the Foundation of Rare Earth Advanced Materials Technology Innovation Center (Grant Nos. CXZX-B-202305-0005 and CXZX-B-202304-0004).

AUTHOR DECLARATIONS

Conflict of Interest

The authors have no conflicts to disclose.

Author Contributions

Jianlong Fu and Dongbo Wang contributed equally to this paper and should be regarded as co-first authors.

Jianlong Fu: Conceptualization (equal); Data curation (equal); Formal analysis (equal); Funding acquisition (equal); Writing – review & editing (equal). **Dongbo Wang**: Data curation (equal); Investigation (equal); Methodology (equal); Visualization (equal); Writing – original draft (equal). **Yan Gao**: Formal analysis (equal); Validation (equal). **Haiyang Yu**: Investigation (equal); Validation (equal). **Deying Zhu**: Validation (equal). **Yanwei Song**: Validation (equal). **Kai Qu**: Validation (equal). **Wenliang Xie**: Visualization (equal). **Yu Wang**: Visualization (equal). **Guozheng Liu**: Project administration (equal); Supervision (equal).

DATA AVAILABILITY

The data that support the findings of this study are available within the article.

REFERENCES

[1] P. P. Mohapatra, G. Li, P. Alagarsamy, and X. Xu, "Advances in grain-boundary diffusion for high-performance permanent magnets," Mater. Futures **3**(4), 042101 (2024).

[2] N. A. Prashanth, "Flux maximization in wind turbine permanent magnet synchronous generator made of NdFeB permanent magnets," Mater. Today: Proc. **49**, 731–737 (2022).

[3] L. Liu, H. Sepehri-Amin, T. Ohkubo, M. Yano, A. Kato, N. Sakuma, T. Shoji, and K. Hono, "Coercivity enhancement of hot-deformed Nd-Fe-B magnets by the eutectic grain boundary diffusion process using $Nd_{62}Dy_{20}Al_{18}$ alloy," Scr. Mater. **129**, 44–47 (2017).

[4] H. Yu, X. Bao, J. Li, and X. Gao, "Microstructure optimization and coercivity enhancement of Nd-Fe-B magnet by double-step diffusion with $Pr_{60}Cu_{20}Al_{20}$ alloy and Tb metal," J. Magn. Magn. Mater. **562**, 169743 (2022).

[5] T.-H. Kim, T. T. Sasaki, T. Koyama, Y. Fujikawa, M. Miwa, Y. Enokido, T. Ohkubo, and K. Hono, "Formation mechanism of Tb-rich shell in grain boundary diffusion processed Nd–Fe–B sintered magnets," Scr. Mater. **178**, 433–437 (2020).

[6] B.-P. Hu, E. Niu, Y.-G. Zhao, G.-A. Chen, Z.-A. Chen, G.-S. Jin, J. Zhang, X.-L. Rao, and Z.-X. Wang, "Study of sintered Nd-Fe-B magnet with high performance of H_{cj} (kOe) + $(BH)_{max}$ (MGOe) >75," AIP Adv. **3**(4), 042136 (2013).

[7] M. Zhang, C. Wang, X. Lü, X. Zhu, Y. Mao, G. Shen, and J. Pan, "Grain boundary diffusion magnet with extremely high comprehensive magnetic properties," J. Chin. Rare Earth Soc. **39**(4), 570–574 (2021).

[8] T. Zhou, J. Chen, Q. Wang, W. Pan, Q. Huang, R. Liu, M. Li, and G. Xie, "Super-high coercivity NdFeB magnet fabricated with double Tb-rich/lean shells by double alloy method and grain boundary diffusion," J. Alloys Compd. **937**, 168368 (2023).

[9] D. Wu, M. Yue, W. Liu, J. Chen, and X. Yi, "Magnetic domain switching in Nd–Fe–B sintered magnets with superior magnetic properties," Mater. Res. Lett. **6**(4), 255–260 (2018).

[10] Z. Jia, Y.-H. Li, X.-T. Yang, S. Cao, G.-F. Ding, S. Guo, X.-D. Fan, Y.-H. Xie, Z.-W. Xiong, R.-J. Chen, and A.-R. Yan, "Strategy of magnetic hardening region regulation enables a record enhanced energy product and high coercivity in Nd-Fe-B magnets," Rare Met. **44**(2), 1267–1283 (2025).

[11] Y. Zhao, H. Feng, A. Li, and W. Li, "Microstructural and magnetic property evolutions with diffusion time in TbHx diffusion processed Nd-Fe-B sintered magnets," J. Magn. Magn. Mater. **515**, 167272 (2020).

[12] E. Yang, W. Jin, C. Man, X. Liu, S. Fu, L. Bo, S. Xu, L. Zhao, Z. Li, Z. Shi, M. Yu, L. Zhao, and X. Zhang, "Evolution of Tb-shell homogeneity in Nd-Fe-B sintered magnets by long-term Tb grain boundary diffusion," J. Alloys Compd. **963**, 171236 (2023).

[13] Z. Lu, T. Wang, F. Lin, J. Jiang, B. Zheng, L. Yang, X. He, J. Li, and Z. Song, "Effect of Al associated grain boundary diffusion of Tb for NdFeB magnets by dual-layer coating," J. Magn. Magn. Mater. **603**, 172240 (2024).

[14] M. Kou, S. Cao, T. Wu, Y. Xie, Z. Jia, H. Luo, X. Fan, G. Ding, B. Zheng, R. Chen, S. Guo, and A. Yan, "Coercivity and thermal stability enhancement of Nd-Fe-B magnet by grain boundary diffusing Tb-Y-La-Cu alloys," J. Alloys Compd. **945**, 169296 (2023).

[15] H. Yu, X. Bao, S. Zha, K. Zhu, S. Guan, Z. Wang, J. Li, and X. Gao, "The dependence of intrinsic coercivity on Tb concentration and core-shell structure of diffused Nd-Fe-B magnets," J. Alloys Compd. **984**, 173917 (2024).

[16] J. He, C. Zeng, L. Zhao, J. Cao, X. Liu, H. Jia, R. Sun, X. Zhang, and Z. Liu, "Boosting efficiency and oxidation resistance of Pr-Tb-Cu diffusion source for Nd-Fe-B magnets by synergistic modification of Al or Ni," Corros. Sci. **237**, 112300 (2024).

[17] J. He, J. Hu, B. Zhou, H. Jia, X. Liu, Z. Zhang, L. Wen, L. Zhao, H. Yu, X. Zhong, X. Zhang, and Z. Liu, "Simultaneous enhancement of coercivity and electric resistivity of Nd-Fe-B magnets by Pr-Tb-Al-Cu synergistic grain boundary diffusion toward high-temperature motor rotors," J. Mater. Sci. Technol. **154**, 54–64 (2023).

[18] D. H. Lee, S. C. Kim, J. Kim, J.-Y. Baek, T.-Y. Yun, J. T. Kim, S. Kim, D. Kim, S. H. Lee, D. Do, D. H. Kim, J. W. Roh, and J. Kim, "Coercivity and thermal stability enhancement of Nd-Fe-B sintered magnets by grain boundary diffusion with Tb-Al-Cu alloys," Materialia **36**, 102161 (2024).

[19] R. Song, H. Zhao, and H. Feng, "Pr–Tb synergistic strengthening on coercivity of Nd-Ce-Fe-B magnets grain boundary diffused with Pr-Tb-Al-Ga alloys," J. Rare Earths **42**(9), 1704–1709 (2024).

[20] C. Li, Y. Xu, G. Li, F. Gao, W. Jiang, Y. Wang, and Y. Xia, "Grain boundary diffusion of sintered NdFeB magnets by TbAl coatings with various Al addition amount," J. Rare Earths (published online) (2024).

[21] P. T. Thanh, N. H. Ngoc, K. X. Hau, N. H. Yen, T. V. Anh, and N. H. Dan, "Coercivity enhancement of sintered Nd–Fe–B magnets by intergranular adding

micro-structured Dy–Nd–Pr–Al–Cu powder," Mater. Trans. **64**(8), 1924–1929 (2023).
[22]T. Zhou, R. Liu, P. Qu, G. Xie, M. Li, and Z. Zhong, "Diffusion behavior and coercivity enhancement of Tb-containing NdFeB magnet by dip-coating TbH_3," J. Mater. Res. Technol. **20**, 1391–1398 (2022).
[23]W. Zhu, Y. Luo, Z. Wang, X. Bai, H. Peng, and D. Yu, "Magnetic properties and microstructures of terbium coated and grain boundary diffusion treated sintered Nd-Fe-B magnets by magnetron sputtering," J. Rare Earths **39**(2), 167–173 (2021).
[24]Q. Yang, R. Wang, Y. Liu, J. Li, H. Chen, and X. Yang, "Coercivity enhancement by low oxygen content graphene addition in hot-deformed Nd-Fe-B magnets," J. Magn. Magn. Mater. **511**, 166940 (2020).
[25]R. Wang, Q. Yang, Y. Liu, J. Li, T. Zhou, and X. Yang, "Coercivity enhancement and microstructural characterization of hot-deformed Nd-Fe-B magnets with graphene addition," Mater. Charact. **178**, 111210 (2021).
[26]Q. Huang, Q. Jiang, J. Hu, S. U. Rehman, G. Fu, Q. Quan, J. Huang, D. Xu, D. Chen, and Z. Zhong, "Extraordinary simultaneous enhancement of the coercivity and remanence of dual alloy HRE-free Nd-Fe-B sintered magnets by post-sinter annealing," J. Mater. Sci. Technol. **106**, 236–242 (2022).
[27]S. Cao, S. Zheng, Z. Jia, Z. Xiong, G. Ding, X. Fan, S. Guo, B. Zheng, R. Chen, C. Yan, and A. Yan, "Coercivity enhancement of NdCeFeB magnet by two-step grain boundary diffusion with $Pr_{70}Cu_{10}Al_{15}Ga_5$ and DyH," J. Alloys Compd. **976**, 173006 (2024).